Available online at www.sciencedirect.com
SCIENCE DIRECT®
Journal of Hydrology 301 (2005) 163–181
Journal of Hydrology
www.elsevier.com/locate/jhydrol

Reductive dissolution of Mn oxides in river-recharged aquifers: a laboratory column study

B.M. Petrunic[a,*], K.T.B. MacQuarrie[a], T.A. Al[b]

[a]*Department of Civil Engineering, University of New Brunswick, P.O. Box 4400, Fredericton, NB, Canada E3B 5A3*
[b]*Department of Geology, University of New Brunswick, P.O. Box 4400, Fredericton, NB, Canada E3B 5A3*

Received 26 November 2002; revised 22 March 2004; accepted 18 June 2004

Abstract

River-recharged aquifers are developed for drinking water supplies in many parts of the world. Often, however, dissolved organic carbon (DOC) present in the infiltrating river water causes biogeochemical reactions to occur in the adjacent aquifer that create elevated Mn and Fe. Mn concentrations in groundwater from some of the production wells installed in the aquifer at Fredericton, New Brunswick exceed the Canadian Drinking Water Guideline of 9.1×10^{-4} mmol/l by up to 5.5×10^{-2} mmol/l. It has previously been hypothesized that the influx of DOC from the Saint John River is causing bacterially mediated reductive dissolution of Mn oxides in the aquifer system, leading to elevated aqueous Mn concentrations. Previous work was limited to the collection of water samples from production wells and several observation wells installed in the glacial outwash aquifer. The objective of this study was to investigate the biogeochemical controls on Mn concentrations using sand-filled columns. One column was inoculated with bacteria while a second column was treated with ethanol in order to decrease the microbial population initially present in the system. Both columns received the same influent solution that contained acetate as a source of DOC. The results of the experiments suggested that the two main controls on Mn concentrations in the columns were microbially mediated reductive dissolution of Mn oxides and cation exchange. The conceptual model that was developed based on the experimental data was supported by the results obtained using a one-dimensional reactive-transport model. The reductive dissolution of Mn oxides in the aquifer sands could be adequately simulated using dual-Monod kinetics. Similar trends are observed in the experimental data and field data collected from Production Well 5, located in the Fredericton Aquifer. From the experiments, it is evident that cation-exchange reactions may be an important geochemical control on Mn concentrations during the initial stages of pumping; however, the reductive dissolution of Mn oxides may represent a long-term source of Mn in the drinking water supply.

Keywords: River-recharged aquifer; Column studies; Manganese; Reductive dissolution; Kinetics

1. Introduction

Aquifers that are hydraulically connected to adjacent rivers have been the focus of several geochemical studies (e.g. Jacobs et al., 1988; Bourg

* Corresponding author. Present address: Department of Geology, University of New Brunswick, P.O. Box 4400, Fredericton, NB, Canada E3B 5A3. Tel.: +1-506-453-4803; fax: +1-506-453-5055.
E-mail address: o0bsn@unb.ca (B.M. Petrunic).

0022-1694/$ - see front matter © 2004 Elsevier B.V. All rights reserved.
doi:10.1016/j.jhydrol.2004.06.022

et al., 1989; von Gunten et al., 1991; Bourg and Bertin, 1993; Doussan et al., 1998). The infiltration of river water into aquifer systems, also referred to as bank filtration, may occur naturally or may be induced by pumping wells installed in the adjacent aquifer. The process of bank filtration usually alters water quality. In general, bank filtration decreases particulates, bacteria, and some inorganic and organic compounds in the bank filtrate, which is beneficial for drinking water supplies (Kuehn and Mueller, 2000). Variations in river water temperature and composition are often dampened in the bank filtrate and as a result the water quality in the aquifer is relatively constant compared to the river (Kuehn and Mueller, 2000). The geochemical evolution of groundwater in aquifers that are hydraulically connected to adjacent rivers depends on the physical and geochemical characteristics of both the river and aquifer systems. Most of these types of systems are similar in that dissolved organic carbon (DOC) present in the infiltrating river water often has a significant effect on the geochemistry in the aquifer.

Thermodynamically, the oxidation of DOC coupled to the reduction of dissolved oxygen (DO), NO_3, Mn(IV), Fe(III), SO_4 or CO_2 is predicted to occur in the order shown in Fig. 1 (Champ et al., 1979). In general, as river water rich in DOC infiltrates into an adjacent aquifer, DO is preferentially consumed. After the depletion of DO, the next available electron acceptor will be consumed according to the sequence shown in Fig. 1, which may lead to the development of discrete redox zones along the infiltration path. Although this is a general expectation, redox processes that occur in groundwater environments are commonly complex and highly site-dependent as shown, for example, by Ludvigsen et al. (1998).

In many river bank filtration water supplies the redox sequence in Fig. 1 proceeds to reaction 3 or 4 creating problems of high Fe or Mn concentrations (e.g. Thomas et al., 1994; Hiscock and Grischek, 2002). Manganese-oxide reductive dissolution is generally thought to occur concurrently with the reductive dissolution of Fe oxides (e.g. Nealson et al., 1989). Lovley (1992) points out the difficulty of differentiating between microbially mediated Mn-oxide reductive dissolution, and the reductive dissolution of Mn oxides by Fe(II) which is generated by

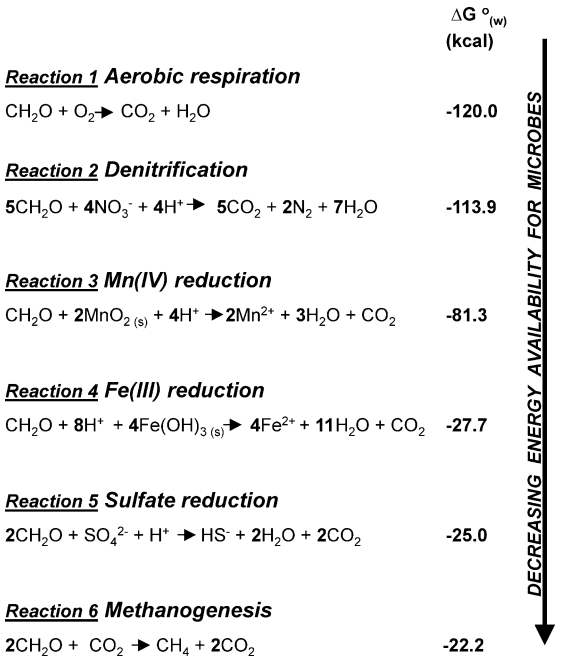

Fig. 1. The thermodynamically predicted order for redox reactions to occur in subsurface environments. In these reactions CH_2O is used to represent labile dissolved organic carbon. The $\Delta G^{o}_{(w)}$ values are determined for a $[H^+]$ of 1×10^{-7} M (Champ et al., 1979).

microbially mediated Fe(III) reduction (reaction 4 in Fig. 1).

The role of microorganisms in the reductive dissolution of both Mn and Fe oxides has been the focus of many studies (e.g. Myers and Nealson, 1988a,b; Lovley et al., 1989). These researchers have investigated the ability of different microorganisms to obtain energy for metabolic processes by coupling the oxidation of various electron donors to Mn(IV) and Fe(III) reduction. The results of many of these studies have been summarized by Lovley (1992). The effect of oxide mineralogy on the microbially mediated reductive dissolution of Mn oxides has also been investigated (Burdige et al., 1992).

In several field-based studies of river-recharged aquifers (e.g. Jacobs et al., 1988; von Gunten et al., 1991; Bourg and Bertin, 1994), elevated Mn concentrations have been observed in the groundwater and have been attributed to the reductive dissolution of Mn oxides (reaction 3 in Fig. 1). In addition, some studies have found that Mn concentrations varied seasonally, with higher concentrations observed in

the summer months (e.g. von Gunten et al., 1991; Bourg and Bertin, 1994). Bourg and Bertin (1994) suggested that the reductive dissolution of Mn oxides in a river-recharged aquifer was microbially mediated and observed that it occurred above a minimum temperature of 10 °C.

In addition to field-based studies, laboratory column experiments have been conducted to assess biogeochemical reactions that occur in river-recharged aquifers (Matsunaga et al., 1993; von Gunten and Zobrist, 1993). Simulated river water was introduced at the influent end of the columns and the geochemical changes that occurred within the sediments were monitored along the length of the columns. These studies assessed a range of redox processes that occurred within the columns as the influent solution, which contained an organic carbon source, travelled through the sediment.

1.1. Background

The Fredericton Aquifer is located in the downtown area of the City of Fredericton, New Brunswick (Fig. 2) and is the primary source of drinking water for the city. Since pumping began in 1955, eight production wells have been installed in the glacial-outwash sand and gravel aquifer (Fig. 2) and currently about 26,000 m^3/d of water is extracted. Manganese concentrations in water from some of the production wells exceed the Canadian Drinking Water Guideline of 9.1×10^{-4} mmol/l (Federal-Provincial Subcommittee on Drinking Water, 1996).

Previous studies have determined that the Fredericton Aquifer and the Saint John River are hydraulically connected (Violette, 1990; Thomas et al., 1994). Thomas et al. (1994) observed a decrease in DOC concentration between the river and Production Well (PW) 5 (Fig. 2). They determined that the degradation of organic carbon due to aerobic and denitrification reactions could not fully account for the observed decrease in DOC concentration. Thomas (1991) hypothesized that Mn oxides that are present in the Fredericton Aquifer undergo reductive dissolution due to the influx of DOC from the Saint John River, resulting in elevated Mn concentrations in the groundwater; however, there are few data available to support this hypothesis. Although temporal changes in river water chemistry could cause subsequent geochemical changes in the aquifer, historical data from the Saint John River suggest that only Na and Cl concentrations have changed significantly since 1961 (Thomas, 1991). Therefore, reactions occurring within the aquifer sediments are likely leading to the geochemical changes observed within the groundwater.

1.2. Objectives

The main objective of this study is to quantitatively assess processes controlling elevated dissolved Mn concentrations in groundwater during bank filtration. Specific objectives include: (1) monitoring temporal geochemical changes that occur as simulated river water infiltrates and interacts with aquifer solids; (2) developing a conceptual model to explain the biogeochemical processes; and (3) simulating the processes occurring in the experimental columns using a one-dimensional reactive-transport model. Since elevated Mn concentrations are often a problematic occurrence at river bank filtration sites, this research should also provide insight that will have applicability to other locations.

2. Methods

2.1. Approach

Geochemical data were obtained from sand-column experiments that were considered to represent a one-dimensional flow path from a river to a well in an adjacent aquifer. The column experiments were conducted using sands from the Fredericton Aquifer (described later). Because Thomas (1991) previously hypothesized that the principal control on Mn concentrations in the Fredericton Aquifer is the reductive dissolution of Mn oxides, batch tests were conducted to determine initial estimates of Mn-oxide reductive dissolution rates and Mn concentrations under various experimental conditions (Petrunic, 2002). These results were then used to design the column experiments and ensure that measurable reductive dissolution of Mn oxides would occur within a reasonable time frame.

The column experiments consisted of monitoring the influent and effluent of two sand-filled columns.

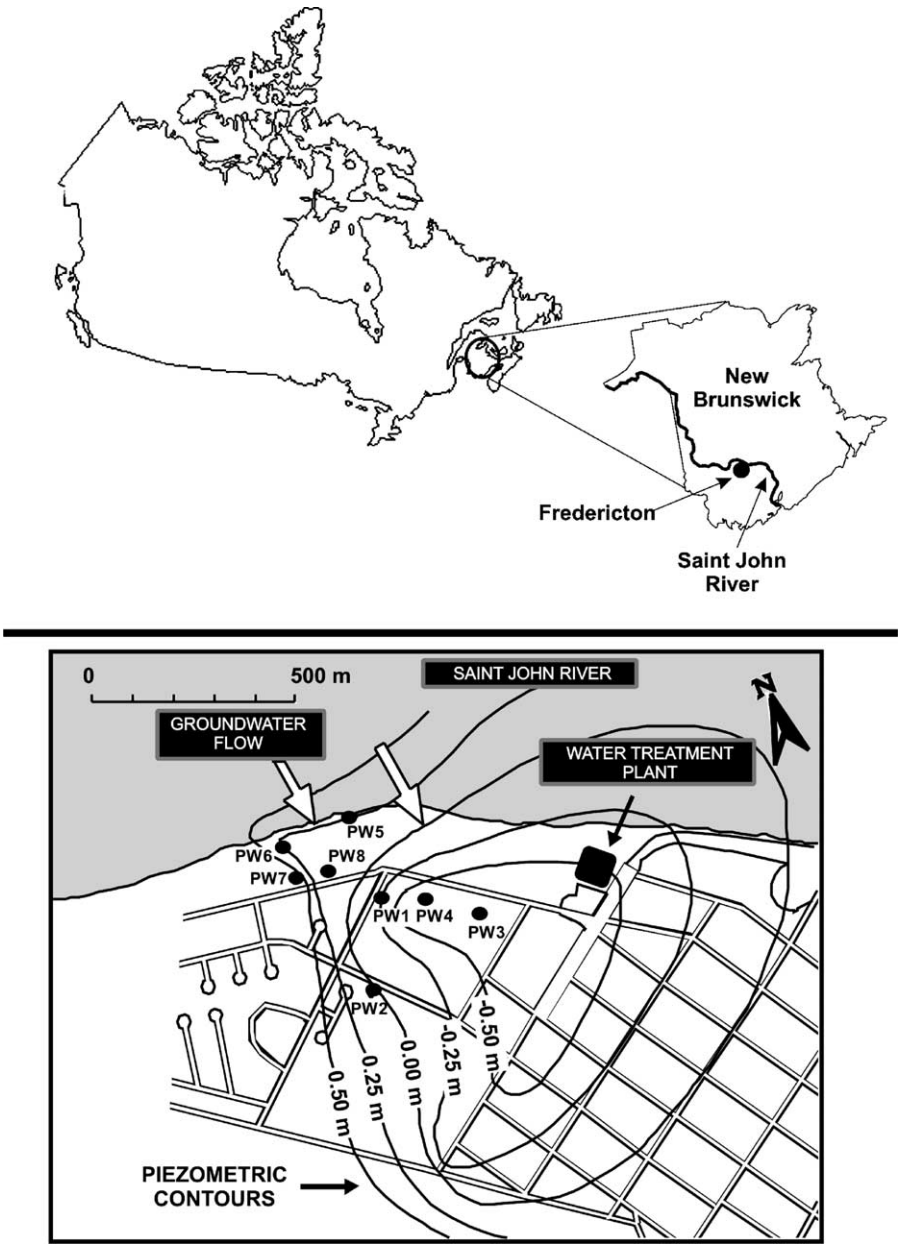

Fig. 2. Location of production wells installed in the Fredericton Aquifer. The piezometric contours are for the aquifer unit in which the wells are screened and the data were collected in 1992, before Production Wells 7 and 8 were installed. The piezometric contour lines represent the hydraulic head relative to sea level, and the river elevation at the time of data collection was 2.2 m.

Because this study was focused on the redox conditions in which Mn oxides are reductively dissolved, the experiments were conducted anaerobically and in the absence of nitrate and sulphate. The influent solution was formulated to be similar to the composition of the Saint John River and contained DOC in the form of acetate. The initial microbial conditions in the two columns differed, making it

possible to assess the importance of microbially mediated Mn-oxide reductive dissolution on Mn concentrations. The aqueous geochemistry in the effluent from both columns was monitored over a 200 day period.

2.2. Experimental set-up

A schematic diagram of the experimental set-up is shown in Fig. 3. The columns were made from plexiglass with an inside diameter of 10.2 cm. The flow path in both columns was 19 cm. The columns were packed with a sand mixture containing 10 wt% pulverized Fredericton Aquifer (FA) sand (source of Mn oxides in the experiments) and 90 wt% silica sand ($<$710 μm). The silica sand was added in order to decrease the initial mass of Mn oxides in the columns thereby decreasing the time for complete Mn oxide depletion. The FA sand was pulverized to ensure a homogeneous distribution of Mn oxides throughout the columns.

In the preliminary batch tests there was evidence that the reductive dissolution of Mn oxides was occurring in tests that did not receive an external source of DOC (Petrunic, 2002). As a result, both sediment samples (FA sand and silica sand) were cleaned with hydrogen peroxide to reduce the amount of organic matter on the surfaces of the sediments (methods modified from Crawford et al., 1998) and to ensure that acetate was the sole electron donor in the column experiments. The FA sand (prior to pulverization) was allowed to sit in a 5% solution of hydrogen peroxide until effervescence diminished (approximately 15 h) whereas the silica sand was allowed to sit in a 20% solution of hydrogen peroxide for approximately 6 h. Both sands were then washed thoroughly with tap water and dried at temperatures between 30 and 40 °C.

The Mn and Fe content of the mixed column sand was determined by extraction with hydroxylamine hydrochloride which preferentially targets the Mn and Fe oxyhydroxide phases of a sediment (Hall et al., 1996). The cation exchange capacity (CEC) of the mixed column sand was determined using a barium chloride ($BaCl_2$) extraction (Hendershot and Duquette, 1986).

In order to observe the effect of microbial mediation, one of the columns (referred to as the 'inoculated column') was inoculated as it was filled with the sand mixture using a microbial population that originated from the Saint John River. The second column (referred to as the 'treated column') was not inoculated; instead a 70% ethanol solution was introduced to the column to decrease the initial microbial population present in the system. In addition, a sterile 0.2 μm flow-through filter was inserted before the inlet of the second column to minimize microbial input from the influent solution.

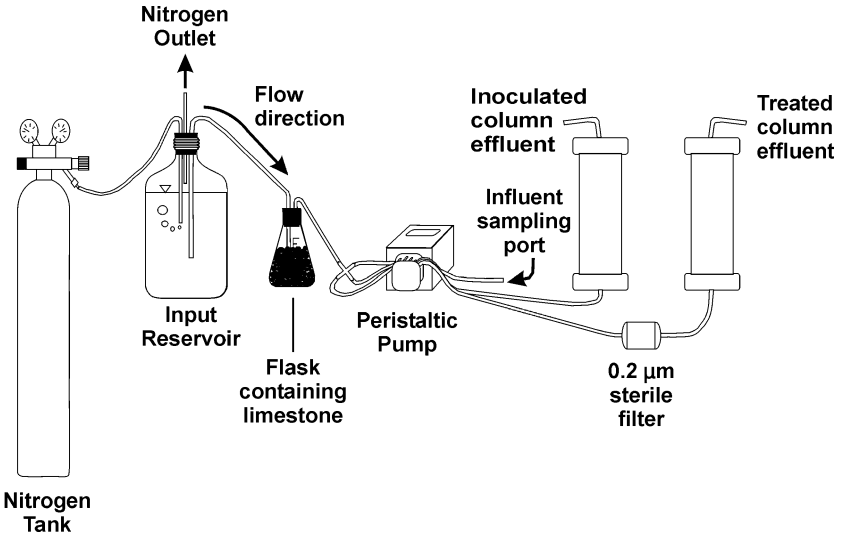

Fig. 3. A schematic diagram of the experimental set-up.

The composition of the influent solution was formulated to be similar to the Saint John River (Table 1). The input solution reservoir was continuously purged with nitrogen gas to remove oxygen (O_2) and prevent aerobic reactions. Bicarbonate alkalinity was added to the input solution by allowing the water to flow through a flask containing crushed limestone.

The source of DOC in the input solution was acetate. All acetate concentrations are reported as mg C/l. The reductive dissolution of Mn oxides (assumed to be present as MnO_2) by acetate is thermodynamically predicted to occur according to the following overall reaction (after Lovley, 1992):

$$CH_3COO^- + 4MnO_2 + 7H^+ \rightarrow 2HCO_3^- + 4Mn^{2+} + 4H_2O \quad (1)$$

The input solution was changed approximately every 4 days to avoid acetate degradation in the input reservoir. In the batch experiments, the highest Mn concentrations were observed in vessels containing FA sand that were incubated at 20 °C. As a result, the column experiments were conducted as close as possible to this temperature (average 23 °C) to ensure that measurable Mn-oxide reductive dissolution would occur.

The volumetric discharge from the columns was measured approximately every 2 weeks. Chloride was used as a conservative tracer to determine the dispersivity and average linear velocity in each column. The dispersivity was determined from the Cl breakthrough data using the program CXTFIT version 2.2 (Toride et al., 1995).

The columns were monitored for a period of 200 days. At day 153, flow to the columns was stopped for 20 days and the columns became closed systems. This was done to determine whether Mn concentrations were limited by mineral precipitation reactions or by reductive-dissolution kinetics (residence time in the column). At day 173, flow to the columns was resumed and the aqueous geochemistry of the effluent from both columns was monitored for another 27 days.

Table 1
Chemical composition of the influent solution used in the experiments and Saint John River water

Parameter	Units	Influent solution		Saint John River		
		Average values	Standard deviation ($n=34$)	Average values[a]	Standard deviation	
					Value	n
pH	–	8.92	0.3	7.7	0.4	23
DOC	mmol/l	n/a	–	0.72	0.14	22
CH_3COO	mmol/l	0.51	0.01	n/a	n/a	n/a
Alkalinity[b]	mmol/l	0.041[c]	0.01	0.41	0.04	21
Ca	mmol/l	0.41	0.01	0.42	0.04	27
Mg	mmol/l	0.082	0.001	0.078	0.007	27
Na	mmol/l	0.48	0.01	0.14	0.02	26
K	mmol/l	0.050	0.001	0.013	0.003	27
Cl	mmol/l	1.3	0.02	0.11	0.02	25
SO_4	mmol/l	<0.005	–	0.073	0.009	25
NO_3	mmol/l	<0.002	–	0.009	0.002	25
Fe	mmol/l	<0.0001	–	0.001[d]	0.0002	15
Mn	mmol/l	<0.0001	–	0.0003[d]	0.0002	13
Cu	mmol/l	<0.0001	–	0.015	0.005	26
Zn	mmol/l	0.0004	0.0004	0.0002[d]	–	1
Sr	mmol/l	0.003	0.0001	n/a	n/a	n/a

n/a, not available.
[a] Data collected in 1998 (K. Dupuis, unpublished data).
[b] Alkalinity as $CaCO_3$.
[c] Alkalinity value determined after acetate alkalinity was subtracted from total alkalinity.
[d] Several samples were not included in the average because the concentrations were below instrument detection.

2.3. Sampling

The influent solution and the effluent of both columns were sampled approximately every 5 days. The volumetric discharge was low (124 ml/d) and, as a result, the average sample collection time was approximately 24 h. Aqueous samples were collected for cation and anion analyses in sample bottles that were first purged with argon gas, then loosely capped during sample collection. The samples were withdrawn into a syringe and immediately filtered (0.1 μm cellulose acetate/nitrate). The cation samples were acidified using concentrated trace-metal nitric acid and stored in a refrigerator until analysis. Anion samples were frozen until analysis. pH and Eh measurements were conducted in sealed syringes using a Ross combination pH electrode (model 815600) and an Orion platinum redox electrode (model 98-78-00). Total alkalinity measurements were determined colourimetrically using a HACH digital titrator and methyl-red bromocresol-green as the indicator. Bicarbonate alkalinity was determined after the contribution from acetate was subtracted from total alkalinity. All sample bottles (high density polyethylene), syringes and filters were acid washed in 10% hydrochloric acid prior to use.

2.4. Analytical methods

The concentrations of Al, As, Ca, Cd, Co, Cr, Cu, Fe, K, Mg, Mn, Na, Ni, Pb, Sr, and Zn were measured using Inductively Coupled Plasma Optical-Emission Spectroscopy (ICP-OES; Spectro Ciros CCD) and selected samples were analysed for As using Graphite Furnace Atomic Absorption Spectroscopy (GF-AAS; Perkin Elmer HGA-400/300). Acetate, SO_4, NO_3 and Cl were determined using Ion Chromatography (IC; Dionex DX-120). A complete list of analyses is provided here, however, only the parameters found in concentrations above detection limits will be discussed.

2.5. Geochemical modelling

The geochemical speciation and reactive-transport model PHREEQC v.2.4.2 (Parkhurst and Appelo, 2001) was used in this study. The model uses an explicit finite difference method to solve the one-dimensional advection–dispersion–reaction equation. The model is capable of incorporating many geochemical processes such as: aqueous geochemical speciation, mineral precipitation–dissolution reactions, exchange reactions, surface-complexation reactions, and kinetic reactions. The model was chosen because of the ability to link aqueous geochemical reactions with one-dimensional transport.

The PHREEQC model was used to determine the geochemical speciation of the influent and effluent aqueous samples collected from both columns and to simulate one-dimensional reactive-transport in the columns to test the conceptual model. The reactive-transport simulations incorporated equilibrium-complexation reactions, cation-exchange reactions, and kinetically controlled Mn-oxide reductive-dissolution reactions. The WATEQ4F database (Ball and Nordstrom, 1991) with the modifications listed in Table 2 was used in all the simulations.

A dual-Monod formulation was used to simulate kinetically controlled Mn-oxide reductive dissolution. The dual-Monod formulation was written in terms of the electron acceptor, which was represented in the model by pyrolusite (MnO_2). The stoichiometry in Eq. (1) was used to represent the reductive dissolution of pyrolusite coupled to the oxidation of acetate.

The Monod formulation for pyrolusite was as follows (square brackets denote concentrations in mol/kg water):

$$\frac{\mathrm{d}[\mathrm{MnO_2}]}{\mathrm{d}t} = -q_{\mathrm{m}} X_{\mathrm{f}} \left(\frac{S_{\mathrm{f}}}{K_{\mathrm{s}} + S_{\mathrm{f}}}\right)\left(\frac{[\mathrm{MnO_2}]}{K_{\mathrm{a}} + [\mathrm{MnO_2}]}\right) \tag{2}$$

where

- q_{m} maximum utilization rate for pyrolusite (mol pyrolusite/(g cells d))
- X_{f} concentration of biomass (g cells/kg water)
- S_{f} concentration of acetate (mol acetate/kg water)
- K_{s} half-saturation constant for acetate (mol acetate/kg water)
- K_{a} half-saturation constant for pyrolusite (mol pyrolusite/kg water).

The corresponding Monod formulation for the biomass in the system was as follows:

Table 2
Modifications made in the WATEQ4F database (Ball and Nordstrom, 1991)

Species or reaction	Resulting change in database
Master species C(−4)	Excluded all the reactions involving methane (CH_4)
Master species C(0)	Included acetate with the following parameters: alkalinity of 0, molecular weight of 59.05 g/mol
Secondary master species	Included the following reaction: $2CO_3^{2-} + 11H^+ + 8e^- = CH_3COO^- + 4H_2O$, $\log k = 49$, $\Delta h = -65.76$ kcal[a]
Association reaction	Included the following reaction: $CH_3COO^- + H^+ = CH_3COOH$, $\log k = 4.76$, $\Delta h = 0$ kcal[b]

[a] Thermodynamic data taken from CRC Handbook of Chemistry and Physics, 78th edition (Lide, 1997).
[b] Thermodynamic data taken from MINTEQ database (Allison et al., 1990).

$$\frac{dX_f}{dt} = kYX_f\left(\frac{S_f}{K_s + S_f}\right)\left(\frac{[MnO_2]}{K_a + [MnO_2]}\right) - bX_f \quad (3)$$

where

k maximum utilization rate for acetate (mol acetate/(g cells d)). Using stoichiometry of Eq. (1) gives $k = 0.25q_m$
Y microbial yield coefficient (g cells/mol acetate)
b first order decay constant (d^{-1}).

The advection–reaction–dispersion equation for acetate in the simulations was represented by the following:

$$\frac{\partial S_f}{\partial t} = D_L\frac{\partial^2 S_f}{\partial x^2} - v\frac{\partial S_f}{\partial x} - kX_f\left(\frac{S_f}{K_s + S_f}\right)\left(\frac{[MnO_2]}{K_a + [MnO_2]}\right) \quad (4)$$

where

D_L hydrodynamic dispersion coefficient (m^2/d)
v pore-water velocity (m/d).

3. Results and discussion

3.1. Geochemical evolution in the columns

The chemical- and physical-transport properties of the sand in the columns are provided in Table 3. The data collected from both columns indicate an initial period when the geochemical conditions were transient, followed by a period of steady-state conditions (Fig. 4A and B). The initial variation in solute concentrations over a time period of approximately 100–120 days is thought to result from variations in the rates of reactions during the establishment of conditions suitable for reductive dissolution of Mn oxides, and from the gradual establishment of cation-exchange equilibrium within the columns. These processes are discussed below in relation to the data.

3.1.1. Transient conditions

The average influent acetate concentration was 0.51 mmol/l (Fig. 4A, Table 1). The initial breakthrough of acetate in the effluent from the inoculated column occurred after approximately 10 days when a concentration of 0.15 mmol/l was reached. From this time until the flow was stopped at 153 days, the concentration of acetate in the inoculated column ranged between 0.15 and 0.21 mmol/l. In contrast, the initial breakthrough of acetate in the effluent from the treated column was similar to the breakthrough of the conservative solute Cl (Fig. 5). Following

Table 3
Properties of the sand in the columns

Parameter	Units	Inoculated column	Treated column
Chemical properties			
Mn	mg/kg sediment	50	50
Fe	mg/kg sediment	569	569
CEC	meq/100 g sediment	0.9	0.9
Physical properties			
Average discharge	ml/d	124	124
Average linear velocity	cm/d	3.54	3.58
Residence time	d	~5	~5
Dispersivity	cm	0.26	0.21

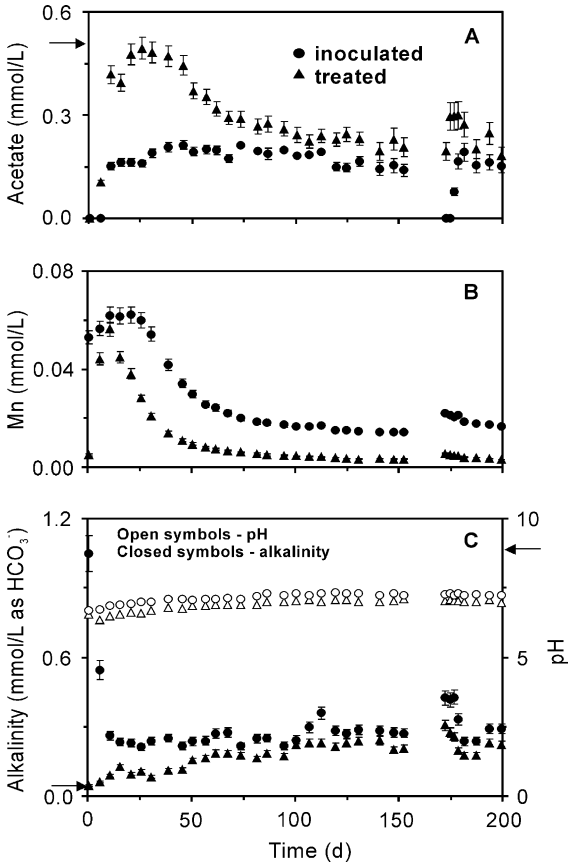

Fig. 4. (A) Acetate concentrations, (B) manganese concentrations, (C) bicarbonate alkalinity values and pH versus time in the effluent from both the inoculated (circles) and treated (triangles) columns. Arrows denote average influent values. Error bars are shown as relative standard deviation of analytical duplicate samples.

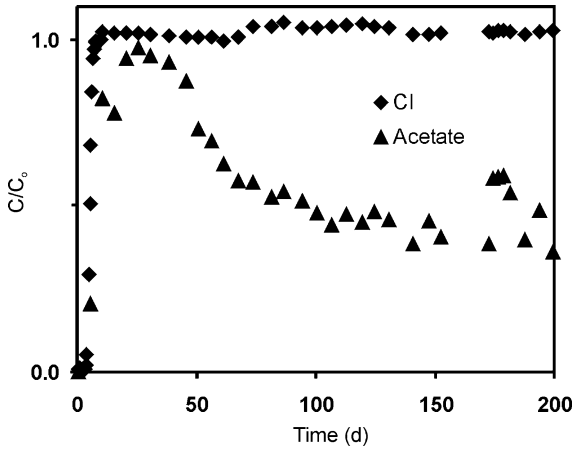

Fig. 5. A comparison between the breakthrough of the conservative anion, Cl (diamonds), and acetate (triangles) in the treated column. The Cl and acetate data were normalized to the average influent concentration.

breakthrough, the acetate concentrations in the treated column remained near influent concentrations until about day 35. Acetate concentrations then declined to a steady-state concentration of about 0.22 mmol/l at approximately 120 days.

Manganese concentrations in the effluent from both columns increased, reaching maximum concentrations within 25 days. The Mn concentrations then declined until steady-state values of 0.015 and 0.0034 mmol/l were reached after approximately 120 days in the effluent from the inoculated and treated columns, respectively (Fig. 4B).

For the inoculated column, the initial lack of acetate and non-zero Mn concentrations in the effluent suggest that the reductive dissolution of Mn oxides occurred as acetate was introduced to the column. In the effluent from the treated column, acetate concentrations did not decrease until about day 35, suggesting that there was a corresponding delay in the onset of Mn(IV) reduction compared to the inoculated column. These inferences are consistent with the observation of higher Mn concentrations in the effluent from the inoculated column, which peaked at 0.062 mmol/l, compared to the Mn concentrations in the effluent from the treated column, which peaked at 0.056 mmol/l. In addition, Mn concentrations in the effluent from the inoculated column remained elevated for a longer period of time (about 15 days) compared to the treated column. The delayed onset of Mn-oxide reductive dissolution in the treated column is most likely a result of the ethanol pretreatment which would have decreased both the microbial population and diversity within the column sediments. The microbial population which survived the ethanol pretreatment would have required additional time for growth, a time period in which, consistent with the data, the consumption of acetate and production of Mn(II) are expected to be low.

The alkalinity data further support the suggestion that Mn-oxide reductive dissolution occurred in both columns but with delayed onset in the treated column (Fig. 4C). The average influent alkalinity concentration was 0.083 mmol/l as bicarbonate (Table 1). The initial alkalinity concentration in the effluent from

the inoculated column was very high (approximately 1.1 mmol/l), then declined to a steady-state value after about 10 days that ranged between 0.21 and 0.36 mmol/l. The initially high alkalinity value in the inoculated column is likely a result of the column being saturated with de-ionized water, followed by a 4-day period without flow prior to beginning the experiment. Under these conditions, the microbial population would be expected to consume any organic carbon available within the column, leading to the observed increase in alkalinity. The higher alkalinity in the effluent from the inoculated column throughout the experiment, compared to the influent solution, is consistent with the oxidation of acetate as in Eq. (1). The alkalinity in the effluent from the treated column started very low (approximately 0.044 mmol/l) and increased to a steady-state concentration of approximately 0.22 mmol/l after 120 days. Similar to the inoculated column, the increasing alkalinity values coupled to decreasing acetate concentrations after 35 days is likely due to the oxidation of acetate.

The reductive dissolution of Mn oxide is a proton consuming reaction and based on the numerical simulations (see below) it is expected that, with the amount of Mn(II) produced in the experiments, the pH in the column effluents would have increased as high as 9.3. This was not the case (Fig. 4C), and the mechanisms contributing to pH buffering within the columns cannot be adequately assessed with the available data. It is possible that other organic-carbon degradation reactions, such as fermentation, contributed to the pH buffering.

Similar to Mn, acetate and alkalinity, the concentrations of the major cations (Ca, K, Mg, and Na) in the effluent from both columns were initially transient, then reached steady-state concentrations at various times (Fig. 6A and B). Sodium concentrations in the effluent from both columns increased steadily to reach the influent concentration after 10 days. Initially, K concentrations increased slightly above the influent concentration during the first 15 days, then declined and stabilized near the influent concentration after 26–30 days. Similarly, Mg concentrations in the effluent from both columns peaked then declined, reaching the influent concentrations after approximately 38 days. Calcium concentrations in the effluent from the inoculated column increased to reach the influent

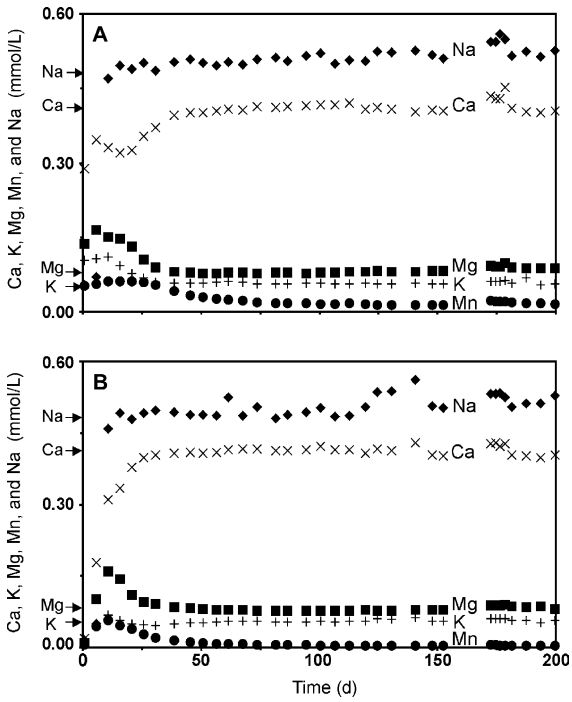

Fig. 6. Cation concentrations in (A) the inoculated column and (B) the treated column versus time. Arrows denote average influent concentrations.

concentration after approximately 46 days, compared to 31 days for the treated column.

The observed trends in cation concentrations in the effluent from both columns are consistent with trends that would be expected as cation-exchange reactions respond to an input solution that is out of equilibrium with the exchange sites in the column sand. The large peaks in Mn concentrations in the columns are thought to result from desorption of Mn(II) from ion-exchange sites in response to the influx of Ca(II) with the influent solution (e.g. Eq. (5) where X represents an exchange site).

$$Ca^{2+} + Mn\text{–}X_2 \rightarrow Mn^{2+} + Ca\text{–}X_2 \quad (5)$$

This inference is supported by the observation that Ca and Mn concentrations approach steady-state within approximately the same time period (Fig. 6). Sodium, K, and Mg reached influent concentrations at similar times in the effluent from both columns, whereas the time required for Ca to reach steady-state concentrations in the inoculated column was greater than in the treated column. In addition, the peak Mn

concentrations remained elevated for a longer period of time in the effluent from the inoculated column compared to the Mn concentrations in the effluent from the treated column. The delays in the establishment of cation-exchange equilibrium are probably related to the reductive dissolution of Mn oxides. The greater mass of Mn on exchange sites within the inoculated column due to the earlier onset of Mn(IV) reduction, is expected to have slowed the progress of Ca–Mn exchange equilibrium along the length of the column.

The progression of cation-exchange reactions within the columns may have been affected by the pretreatment of the aquifer sand with hydrogen peroxide. The pretreatment could have caused the oxidation of adsorbed Mn(II) (naturally present on the sands) or reductive dissolution of the Mn oxides (Nealson et al., 1989). If the oxidation of Mn(II) occurred on the mineral surfaces during the pretreatment, the observed Mn peak may be suppressed. Alternatively, if the Mn oxides were reductively dissolved during the pretreatment, the Mn peak may have been enhanced. Unfortunately, the effect that the pretreatment had on the aquifer material is unknown, but the onset of Mn-oxide reductive dissolution in the columns would undoubtedly cause cation-exchange reactions to occur in both columns.

3.1.2. Steady-state conditions

After approximately 120 days, near steady-state conditions were reached for all parameters in both columns. With the exception of Mn, steady-state concentrations for the major cations were similar to the respective average cation concentrations in the influent solution. Manganese was not detected in the influent solution; however, the concentrations of Mn remained elevated in the effluent from both columns after other cations reached steady-state values. This supports the suggestion that reductive dissolution of Mn oxides provided an internal source of Mn.

Average steady-state concentrations for Mn were higher in the effluent from the inoculated column (0.015 mmol/l) compared to the effluent from the treated column (0.003 mmol/l) (Fig. 4B). The average acetate concentrations at steady-state were 0.15 and 0.22 mmol/l in the effluent from the inoculated and treated columns, respectively (Fig. 4A), a decrease of approximately 0.3–0.4 mmol/l compared to the influent solution. At steady-state, the consumption of approximately 0.4 mmol/l of acetate (as carbon) should yield approximately 0.8 mmol/l of Mn according to the stoichiometry in Eq. (1). Manganese concentrations did not reach these expected values and there are two possible explanations for the observed difference: (1) Mn(II) concentrations were limited by mineral precipitation reactions; and (2) the acetate was not solely consumed by the reaction presented in Eq. (1).

Lovley and Phillips (1988a) identified rhodochrosite in laboratory experiments after Mn oxides were reductively dissolved by acetate in the presence of the bacteria GS-15. The precipitation of rhodochrosite was also believed to limit Mn(II) concentrations in laboratory column experiments that were used to assess biogeochemical processes in a river-recharged aquifer (Matsunaga et al., 1993). The role of precipitation reactions in controlling the steady-state Mn(II) concentrations observed in the present study has been assessed with geochemical modelling. Saturation indices calculated with PHREEQC indicate that the porewater in the columns was undersaturated with respect to rhodochrosite suggesting that rhodochrosite precipitation did not limit Mn(II) concentrations in these experiments.

The issue of whether the Mn concentrations in the effluent from the columns was limited by mineral precipitation reactions, or alternatively, by the kinetic rate of Mn-oxide reductive dissolution, was further investigated by stopping flow through the columns at day 153 in order to increase the residence time. When flow was resumed on day 173, the concentrations of Mn in the effluent increased for both columns (Fig. 4B). This observation indicates that the reductive dissolution reaction rate, rather than Mn-mineral precipitation, was the limiting factor for the Mn concentrations in the effluent.

Since Mn concentrations were not attenuated by precipitation reactions, the excess acetate consumption must be explained by processes other than Mn-oxide reductive dissolution. It is possible that acetate was consumed by fermentation reactions according to, for example, the following reaction:

$$CH_3COO^- + H^+ \rightarrow CO_2 + CH_4 \quad (6)$$

In order to assess the controls on acetate concentrations within both columns, carbon mass balance calculations were performed. From these calculations the fraction of acetate that was utilized for Mn-oxide reductive dissolution reactions was determined and the fate of the remaining acetate was deduced. The calculations were performed using the steady-state data collected from both columns (Table 4).

The following assumptions were made for the calculations:

(1) the reductive dissolution of Mn oxides occurred according to Eq. (1),
(2) the fermentation of acetate occurred according to Eq. (6),
(3) mineral-precipitation and dissolution reactions did not consume or produce bicarbonate within the two columns,
(4) the amount of acetate consumed in the columns is equal to the influent mass flux minus the effluent mass flux,
(5) the amount of bicarbonate produced in the columns is equal to the effluent mass flux minus the influent mass flux, and
(6) Fe-oxide reductive dissolution, denitrification and sulphate reduction did not occur.

The calculations indicate that only 2 and 1% of the total acetate consumed in the inoculated and treated columns, respectively, can be accounted for by the reductive dissolution of Mn oxides. Similarly, only 4 and 1% of the total bicarbonate produced in the inoculated and treated columns, respectively, can be accounted for by the reductive dissolution of Mn oxides. Furthermore, if the remaining mass of acetate was degraded by fermentation according to Eq. (6), 79 and 87% of the total bicarbonate produced can be accounted for in the inoculated and treated columns, respectively. These calculations suggest that there was a source of bicarbonate in the columns that cannot be accounted for by Eqs. (1) and (6). The source of this bicarbonate is not certain. Geochemical modelling results suggest that the effluent from both columns was undersaturated with respect to most carbonate minerals, therefore, carbonate-mineral dissolution may account for the excess bicarbonate. It is also likely that acetate degradation was more complex than is suggested by Eq. (6). For instance, some of the carbon that is reduced to form methane (CH_4), according to Eq. (6), may actually be converted to bicarbonate.

Table 4
Data used in the carbon mass balance calculations

Parameter (mmol/l)	Influent solution (average)	Inoculated column effluent[a]	Treated column effluent[a]
Bicarbonate	0.083±0.02	0.28±0.007	0.22±0.02
Acetate	0.51±0.01	0.15±0.009	0.22±0.02
Mn	–	0.015±0.0004	0.0034±0.0002

[a] Average value between 120 and 153 days.

The steady-state acetate and Mn concentrations were different in the two columns, indicating that the Mn-oxide reductive dissolution rates were not the same. The difference in rates is also evident from the differences in Mn and acetate concentrations in the column effluent after flow to the columns was interrupted between 153 and 173 days. When flow was resumed, Mn concentrations in the effluent from the inoculated column increased by 7.6×10^{-3} mmol/l compared to an increase of only 2.2×10^{-3} mmol/l in the effluent from the treated column (Fig. 4B). The acetate concentrations in the effluent from the inoculated column declined to non-detectable values during the period when flow was stopped, whereas acetate concentrations in the effluent from the treated column actually increased. These differences in Mn(II) production rates and acetate consumption suggest there were significant differences in the microbial ecology in the columns, probably as a result of the initial ethanol treatment.

Although the above discussion pertains mainly to the microbially mediated reductive dissolution of Mn oxides coupled to the oxidation of DOC, it is possible that other reactions contributed to the elevated concentrations of Mn(II) in the column effluents. For example, Nealson et al. (1989) suggest that both Mn- and Fe-oxide reductive dissolution should be considered together. Lovley and Phillips (1988b) found that the microorganism GS-15 did not preferentially reduce Mn oxides in the presence of Fe oxides as may be expected thermodynamically, rather both reactions occurred at the same time. Since the column sand contains appreciable amounts of Fe oxides it may be expected that Mn- and Fe-oxide reductive dissolution

occurred concurrently. As such, the lack of measurable Fe concentrations in the effluent from the columns was likely due to the abiotic reductive dissolution of Mn oxides by Fe(II) as suggested by Lovley and Phillips (1988b). The lack of Fe in the effluent of the columns is supported by mass balance calculations which suggest that only 27 and 11% of the total Mn (assumed to be present as Mn oxides) in the inoculated and treated columns, respectively, was removed during the course of the experiment. Although some of the Mn oxides that remained may not have been reducible, the presence of Mn in the effluent from both columns at steady state suggests that reducible Mn oxides still existed in the columns.

3.2. Conceptual model

A conceptual model was developed to describe the processes that occurred in the columns. The important elements of the conceptual model are described below, and these represent the basis of the numerical model development.

- Bacterially mediated reductive dissolution of the oxides represents a source for dissolved Mn(II) within the columns.
- At the start of the experiment, exchangeable Mn(II) occurs on the surfaces of the column materials.
- During the initial transient period, Mn(II) concentrations are controlled by cation-exchange reactions.
- During the steady-state period, Mn(II) concentrations are controlled by the rate of Mn-oxide reductive-dissolution reactions.
- Reductive-dissolution reactions account for a very small fraction of the total acetate degraded (1–2%).

3.3. Reactive-transport modelling of column results

Reactive-transport simulations were performed to further test the conceptual model. In the first set of simulations, aqueous speciation and equilibrium cation-exchange reactions were included as geochemical controls. The second set of transport simulations included aqueous speciation, equilibrium cation-exchange reactions, and kinetically controlled Mn-oxide reductive dissolution.

The average influent composition presented in Table 1 was used to define the influent solution in the simulations. The initial conditions within the columns were represented by the composition of the first effluent samples collected from the columns at 0.6 days. Cauchy boundaries (i.e. flux-type) were specified at both the inflow and outflow of the simulated columns. A Cauchy-type boundary is justified for the inflow boundary because, as noted by Parkhurst and Appelo (2001), the diameter of inlet tubing (0.3 cm) for the experiments was significantly smaller than the diameter of the columns (10.2 cm). Similarly, Appelo and Postma (1996) suggest that a flux-type boundary is the most suitable boundary condition to use in order to describe breakthrough curves at the outflow of a laboratory column. A summary of the key parameters used in the transport simulations is presented in Table 5.

The model Peclet and Courant values were determined from the criteria specified by Bear and Verruijt (1987). The Peclet numbers in the inoculated and treated columns were 0.96 and 1.19, respectively. The Courant numbers in both columns were equal to 1.

3.3.1. Simulations without reductive dissolution of Mn oxides

Reaction and transport were simulated using equilibrium aqueous speciation and cation-exchange reactions, excluding the reductive dissolution of Mn oxides (Figs. 7 and 8). A CEC value of 0.004 eq/kg

Table 5
Parameters used in the transport simulations

Parameter	Units	Inoculated column	Treated column
Velocity	cm/d	3.54	3.58
Dispersivity	cm	0.26	0.21
Porosity	–	0.43	0.43
Molecular diffusion coefficient	cm^2/d	0	0
Concentration of pyrolusite	mol/kg water	3.95×10^{-3}	3.95×10^{-3}
Model time step	s	6102	6034
Model cell length	cm	0.25	0.25
Number of cells	–	76	76

water was used for the simulations. This CEC value was determined by fitting the cation data collected from the treated column within the first 25 days of the experiment since reductive dissolution of Mn oxides did not occur in the treated column during this time. The CEC value of 0.04 eq/kg water (0.9 meq/100 g sediment) determined by extraction with $BaCl_2$ is 10 times greater than the CEC value determined from the model fit. Jardine et al. (1988) found that adsorption isotherms measured in batch experiments over-estimated solute retardation in soil columns which contained undisturbed sediments. However, Valocchi et al. (1981) found that batch-determined chemical parameters (i.e. selectivity coefficients and ion-exchange capacity) could be used to adequately

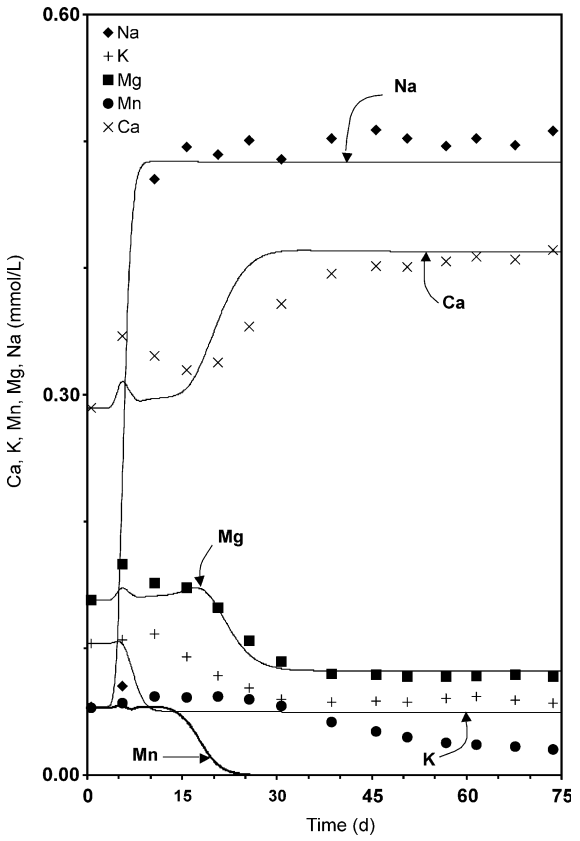

Fig. 7. Measured (symbols) and simulated (solid lines) cation concentrations in the effluent from the inoculated column versus time. The model results are from simulations in which equilibrium cation-exchange reactions were included, but Mn-oxide reductive dissolution was excluded.

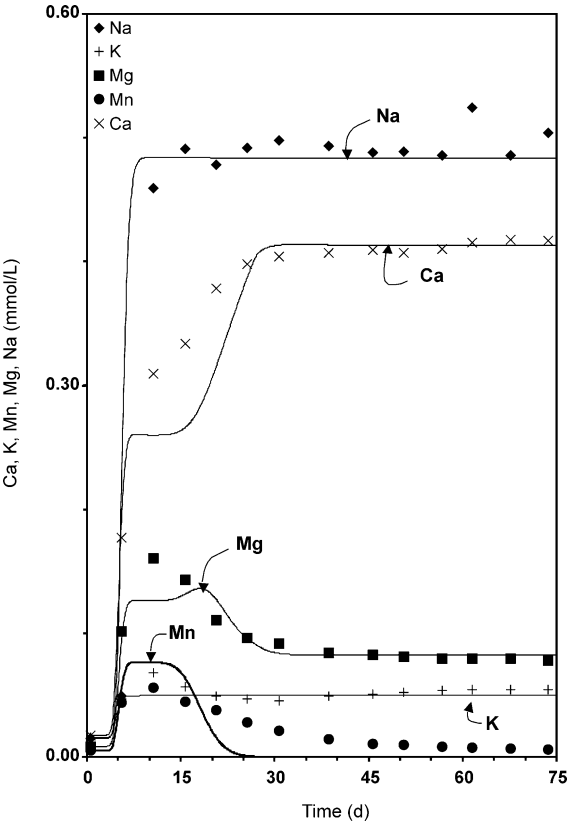

Fig. 8. Measured (symbols) and simulated (solid lines) cation concentrations in the effluent from the treated column versus time. The model results are from simulations in which equilibrium cation-exchange reactions were included, but Mn-oxide reductive dissolution was excluded.

simulate field data. The discrepancy between the batch-determined CEC and the model-determined CEC values may occur due to: (1) preferential flow paths in the columns; and/or (2) selectivity coefficients in the WATEQ4F database (Ball and Nordstrom, 1991) that do not represent the experimental system. In addition, there are a variety of experimental methods that can be used to determine the CEC of sediments and depending on the conditions (e.g. pH and equilibration time) the experimentally determined CEC value may vary.

The results from the numerical simulations demonstrate that cation-exchange reactions can replicate the variation observed in most of the major cation concentrations (Figs. 7 and 8). However, in contrast to the experimental results, the simulated Mn

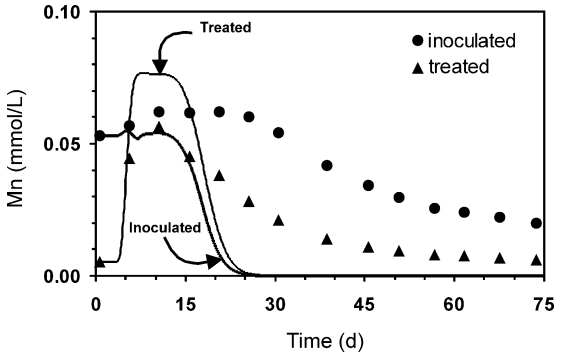

Fig. 9. Measured (symbols) and simulated (solid lines) Mn concentrations in the effluent from both the inoculated and treated columns versus time. The model results are from transport simulations in which equilibrium cation-exchange reactions were considered.

concentrations decline to zero after about 25–30 days (Fig. 9). This suggests that another process is required in the model to reproduce the persistent non-zero Mn concentrations.

3.3.2. Simulations that include reductive dissolution of Mn oxides

The Mn data from the effluent of both columns could be reproduced more closely with the model by including kinetically controlled reductive dissolution of Mn oxides with cation-exchange reactions and geochemical speciation (Fig. 10). The Mn data from the treated column was reproduced by trial and error adjustment of the key Monod parameters. The Monod parameters obtained by fitting the data from the treated column were then used to simulate the inoculated column, with the only difference between the simulations being a different initial biomass concentration. In order to achieve a reasonable fit to the Mn(II) concentrations, the initial biomass ($X_f(t=0)$) in the inoculated column needed to be approximately twice the initial biomass used to simulate the results from the treated column. The relative initial biomass values are consistent with the experimental procedures that were followed. Prior to beginning the experiment microbes were added to the inoculated column, whereas an attempt was made to reduce the initial microbial population present in the treated column.

The results shown in Fig. 10 clearly indicate that Mn-oxide reductive dissolution is required to

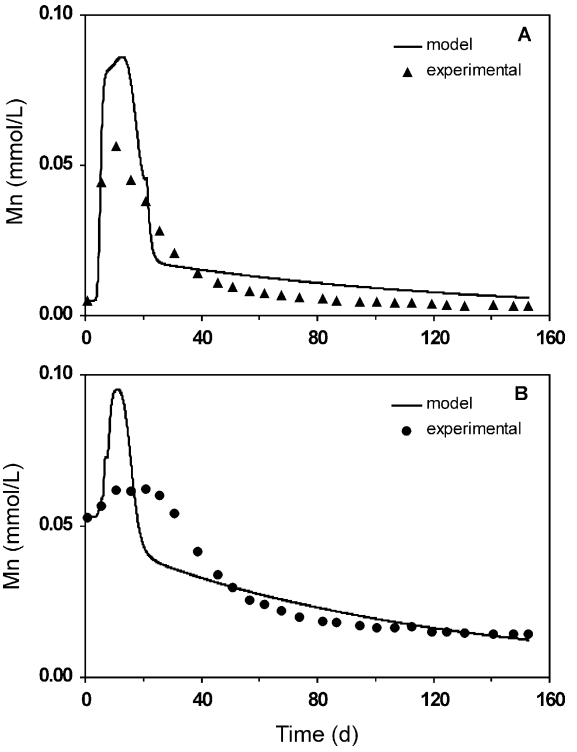

Fig. 10. The results of transport simulations for (A) the treated column and (B) the inoculated column. Simulations included aqueous speciation, equilibrium cation-exchange reactions and kinetically controlled Mn-oxide reductive dissolution.

maintain the long-term Mn concentrations that were observed in the columns. In addition, there was no significant decrease in the simulated acetate concentrations (data not shown) which is consistent with the results of the carbon mass balance calculations that suggest Mn-oxide reductive dissolution could not have accounted for all the acetate degradation observed in the column experiments.

A limited sensitivity analysis was performed to constrain the Monod parameters that were used for the simulations. The sensitivity analysis was only preformed for the inoculated column as it is expected that similar results would be obtained for the treated column. Similar to Chen et al. (1992), the sensitivity of the model results was assessed by varying one parameter (i.e. k, K_s, $X_f(t=0)$, Y, or b) while keeping the remaining parameters fixed. The model results are very sensitive to k and K_s, with a slight increase or decrease in these values resulting in unacceptable

comparisons to the experimental Mn results. For example, increasing k by a factor of two, or lowering K_s by a factor of two, resulted in simulated maximum Mn concentrations of about 0.4 mmol/l, which significantly exceeds the observed peak Mn concentrations (Fig. 4B). In contrast, varying the initial biomass ($X_f(t=0)$) or death rate (b) by an order of magnitude did not cause any major changes to the simulated results for the early-time Mn data (i.e. <10 days); however, such values did not produce a good fit to the measured Mn concentrations at later times. Similarly, a higher or lower yield coefficient (Y) did not affect the model fit for the early-time Mn data but resulted in a poor fit to the Mn concentrations at times exceeding 25 days. The reasonable comparison between the calibrated Monod parameters and those obtained in other studies (Table 6) that have used acetate as an electron donor, also gives greater confidence in the kinetic parameters.

3.4. Comparison of experimental data with historical field data

Prior to the installation of the first pumping well in the Fredericton Aquifer in 1955, the City of Fredericton obtained drinking water directly from the Saint John River. It is expected that the installation of pumping wells in the aquifer caused a reversal in the natural water table gradient and resulted in sustained infiltration of river water into the aquifer.

Production Well 5 is located approximately 20 m from the Saint John River (PW5, Fig. 2) and the average pumping rate from the well is 3650 m^3/d. Due to the close proximity of the well to the river and the large pumping rate, the river acts as the major source of recharge to the well. The concentration history of water from PW5 may therefore have evolved according to the redox sequence shown in Fig. 1, with elevated Mn concentrations resulting from cation exchange and reductive dissolution of Mn oxides. As a result, a qualitative comparison between the trends in Mn concentrations from PW5 and the experimental data can be made. The temporal trends in Mn concentrations that were observed in the experimental results are similar to the trend observed for Mn concentrations in PW 5 (Fig. 11). Although the time scale, flow dimensionality, seasonal variability and aquifer heterogeneity differ significantly between the laboratory and field flow paths, the mechanistic understanding that is obtained from the column experiments suggests that the large initial peak in the Mn concentrations from the city well may be explained primarily by cation-exchange reactions. By analogy with the experimental results, it would be expected that a longer-term steady-state period of lower Mn concentrations will occur in the future due to the continued reductive dissolution of Mn oxides.

4. Conclusions

It was possible to identify two major controls on Mn concentrations in the column systems:

Table 6
The Monod parameters determined from the experiments compared to literature values

Monod parameter	Units	Experimental value	Value from Williamson and McCarty (1976)	Value from Rittmann and McCarty (1980)[a]
K_s	mol acetate/kg water	1×10^{-3}	1.5×10^{-2}	6.6×10^{-5}
$k=0.25q_m$	mol acetate/(g cells d)	0.013	0.080	0.18
X_f (initial)—treated column	g cells/kg water	4.5×10^{-4}	n/a	n/a
X_f (initial)—inoculated column	g cells/kg water	1.0×10^{-3}	n/a	n/a
Y	g cells/mol acetate	30	n/a	7.9
b	d^{-1}	0.09	n/a	0.20

(1) The value of K_a is not reported because the moles of pyrolusite consumed in the simulations was negligible, thus the K_a value did not influence the results of the simulations and was not used as a fitting parameter. (2) n/a, not available.

[a] To convert the Monod parameters reported by Rittmann and McCarty (1980) from units containing 'g of carbon' to units of 'g of cells', the 'cells' or biomass in the simulations was represented by the chemical formula $C_5H_7O_2N$ which was previously defined by Rittmann and VanBriesen (1996) (i.e. there are 60.05 g of C for every 1 mol of cells; MW 113 g cells/mol cells).

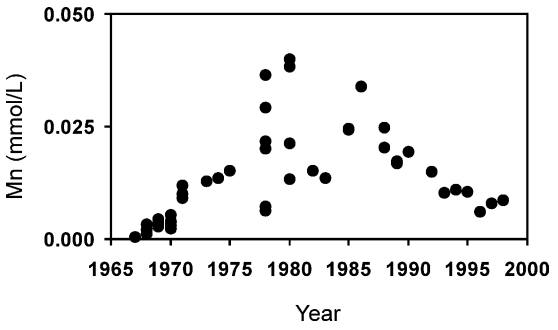

Fig. 11. Manganese concentrations in PW 5 located in the Fredericton Aquifer. The well is located approximately 20 m from the Saint John River, with a vertical well screen that extends from approximately 15 to 24 m below the river bed.

cation-exchange reactions and microbially mediated reductive dissolution of Mn oxides.

The concentrations of the cations (Ca, K, Na, Mg, and Mn) in the effluent from both columns were initially transient, with trends consistent with cation-exchange. With the exception of Mn, the concentrations of all other cations reached influent concentrations after about 46 days, indicating that cation-exchange equilibrium had been established. Although Mn was not present in the influent solution, Mn concentrations remained elevated in the effluent from both columns at steady-state indicating that Mn(II) was released from the sediments through reductive dissolution of Mn oxides. The comparison of data between the inoculated and the treated column clearly indicates that the reductive dissolution of Mn oxides was microbially mediated.

Reductive dissolution of Mn oxides occurred immediately with the introduction of acetate to the inoculated column and was delayed for approximately 35 days in the treated column. The delay in the treated column resulted from the ethanol treatment and probably represents the time required to re-establish a viable Mn-oxide reducing bacterial population.

Acetate consumption associated with microbially mediated reductive dissolution of Mn oxides in the column systems could account for only a small fraction of the total acetate degraded. The majority of the acetate in the columns was likely consumed by fermentation reactions as suggested by the carbon mass balance calculations. The bicarbonate in the effluent from the columns remained above the influent concentration which is consistent with the oxidation of acetate by either reductive dissolution of Mn oxides or fermentation reactions. Although bicarbonate was produced in the columns, carbonate-mineral precipitation reactions were not a limitation to cation concentrations.

The early-time experimental data displayed a trend similar to data collected from a river bank production well, suggesting that cation-exchange processes may contribute significant amounts of Mn to the groundwater over time periods of decades. Elevated Mn concentrations in the aquifer have previously been attributed to reductive dissolution processes alone (Thomas, 1991; Thomas et al., 1994). By analogy with the experimental results it may be expected that after initial exchange reactions have reached equilibrium, Mn concentrations exceeding 9.1×10^{-4} mmol/l will persist due to Mn-oxide reductive dissolution if reducible Mn oxides and labile DOC are available.

Acknowledgements

The authors would like to thank the Natural Sciences and Engineering Research Council of Canada for providing funding for the project through the operating grants awarded to Dr. Kerry MacQuarrie and Dr. Tom Al at the University of New Brunswick, Fredericton, Canada. The authors also wish to thank the City of Fredericton for providing assistance during the collection of aquifer sand samples that were used for the project. The authors thank the three reviewers for their constructive comments on an earlier version of the manuscript.

References

Allison, J.D., Brown, D.S., Novo-Gradac, K.J., 1990. MINTEQA2/PRODEFA2—A Geochemical Assessment Model for Environmental Systems—version 3.0 User's Manual. Environmental Research Laboratory, Office of Research and Development, US Environmental Protection Agency, Athens, Georgia.

Appelo, C.A.J., Postma, D., 1996. Geochemistry, groundwater and pollution. Balkema, Rotterdam.

Ball, J.W., Nordstrom, D.K., 1991. WATEQ4F—User's manual with revised thermodynamic data base and test cases for

calculating speciation of major, trace and redox elements in natural waters. US Geological Survey Open-File Report 90-129.

Bear, J., Verruijt, A., 1987. Modeling groundwater flow and pollution. Reidel, Boston, MA.

Bourg, A.C.M., Bertin, C., 1993. Biogeochemical processes during the infiltration of river water into an alluvial aquifer. Environ. Sci. Technol. 27, 661–666.

Bourg, A.C.M., Bertin, C., 1994. Seasonal and spatial trends in manganese solubility in an alluvial aquifer. Environ. Sci. Technol. 28, 868–876.

Bourg, A.C.M., Darmendrail, D., Ricour, J., 1989. Geochemical filtration of riverbank and migration of heavy metals between the Deûle River and the Ansereuilles Alluvion-Chalk Aquifer (Nord, France). Geoderma 44, 229–244.

Burdige, D.J., Dhakar, S.P., Nealson, K.H., 1992. Effects of manganese oxide mineralogy on microbial and chemical manganese reduction. Geomicrobiol. J. 10, 27–48.

Champ, D.R., Gulens, J., Jackson, R.E., 1979. Oxidation–reduction sequences in groundwater flow systems. Can. J. Earth Sci. 16, 12–23.

Chen, Y.-M., Abriola, L.M., Alvarez, P.J.J., Anid, P.J., Vogel, T.M., 1992. Modeling transport and biodegradation of benzene and toluene in sandy aquifer material: comparisons with experimental measurements. Water Resour. Res. 28 (7), 1833–1847.

Crawford, J.J., Traina, S.J., Tuovinen, O.H., 1998. Biodegradation of benzoate with nitrate as electron acceptor at different redox potentials in sand column microcosms. Biol. Fertil. Soils 27, 71–78.

Doussan, C., Ledoux, E., Detay, M., 1998. River-groundwater exchanges, bank filtration, and groundwater quality: ammonium behaviour. J. Environ. Qual. 27, 1418–1427.

Federal-Provincial Subcommittee on Drinking Water of the Federal-Provincial Committee on Environmental and Occupational Health, 1996. Guidelines for Canadian Drinking Water Quality, 6th ed. Canada Communication Group, Ottawa, Canada.

Hall, G.E.M., Vaive, J.E., Beer, R., Hoashi, M., 1996. Selective leaches revisited, with emphasis on the amorphous Fe oxyhydroxide phase extraction. J. Geochem. Explor. 56, 59–78.

Hendershot, W.H., Duquette, M., 1986. A simple barium chloride method for determining cation exchange capacity and exchangeable cations. Soil Sci. Soc. Am. J. 50, 605–608.

Hiscock, K.M., Grischek, T., 2002. Attenuation of groundwater pollution by bank filtration. J. Hydrol. 266, 139–144.

Jacobs, L.A., von Gunten, H.R., Keil, R., Kuslys, M., 1988. Geochemical changes along a river-groundwater infiltration flow path: Glattfelden, Switzerland. Geochim. Cosmochim. Acta 52, 2693–2706.

Jardine, P.M., Wilson, G.V., Luxmoore, R.J., 1988. Modeling the transport of inorganic ions through undisturbed soil columns from two contrasting watersheds. Soil Sci. Soc. Am. J. 52, 1252–1259.

Kuehn, W., Mueller, U., 2000. Riverbank filtration, an overview. J. Am. Water Works Assoc. December, 60–69.

Lide, D.R. (Ed.), 1997. CRC Handbook of Chemistry and Physics, 78th ed. CRC Press, Boca Raton.

Lovley, D.R., 1992. Microbial oxidation of organic matter coupled to the reduction of Fe (III) and Mn (IV) oxides, in: Skinner, H.C.W., Fitzpatrick, R.W. (Eds.), Catena Supplement 21, Biomineralization, Processes of Iron and Manganese, Modern and Ancient Environments. Catena Verlag, Cremlingen-Destedt, Germany, pp. 101–114.

Lovley, D.R., Phillips, E.J.P., 1988a. Novel mode of microbial energy metabolism: organic carbon oxidation coupled to dissimilatory reduction of iron or manganese. Appl. Environ. Microbiol. 54 (6), 1472–1480.

Lovley, D.R., Phillips, E.J.P., 1988b. Manganese inhibition of microbial iron reduction in anaerobic sediments. Geomicrobiol. J. 6, 145–155.

Lovley, D.R., Phillips, E.J.P., Lonergan, D.J., 1989. Hydrogen and formate oxidation coupled to dissimilatory reduction of iron or manganese by *Alteromonas putrefaciens*. Appl. Environ. Microbial. 55 (3), 700–706.

Ludvigsen, L., Albrechtsen, H.-J., Heron, G., Bjerg, P.L., Christensen, T.H., 1998. Anaerobic microbial redox processes in a landfill leachate contaminated aquifer (Grindsted, Denmark). J. Contam. Hydrol. 33, 273–291.

Matsunaga, T., Karametaxas, G., von Gunten, H.R., Lichtner, P.C., 1993. Redox chemistry of iron and manganese minerals in river-recharged aquifers: a model interpretation of a column experiment. Geochim. Cosmochim. Acta 57, 1691–1704.

Myers, C.R., Nealson, K.H., 1988a. Bacterial manganese reduction and growth with manganese oxide as the sole electron acceptor. Science 240, 1319–1321.

Myers, C.R., Nealson, K.H., 1988b. Microbial reduction of manganese oxides: interactions with iron and sulfur. Geochim. Cosmochim. Acta 52, 2727–2732.

Nealson, K.H., Rosson, R.A., Myers, C.R., 1989. Mechanisms of oxidation and reduction of manganese, in: Beveridge, T.J., Doyle, R.J. (Eds.), Metal ions and Bacteria. Wiley, New York, NY, pp. 383–411.

Parkhurst, D.L., Appelo, C.A.J., 2001. User's guide to PHREEQC (version 2)—a computer program for speciation, batch-reaction, one-dimensional transport, and inverse geochemical calculations. US Geological Survey Water-Resources Investigations Report 99-4259.

Petrunic, B.M., 2002. Reductive dissolution of manganese oxides in river-recharged aquifers: laboratory-scale investigations. MScE Thesis, University of New Brunswick, Department of Civil Engineering, Fredericton, NB, Canada.

Rittmann, B.E., McCarty, P.L., 1980. Evaluation of steady-state-biofilm kinetics. Biotechnol. Bioeng. 22, 2359–2373.

Rittmann, B.E., VanBriesen, J.M., 1996. Microbiological processes in reactive modeling, in: Lichtner, P.C., Steefel, C.I., Oelkers, E.H. (Eds.), Reactive Transport in Porous Media Reviews in Mineralogy, vol. 34. The Mineralogical Society of America, Washington, DC, pp. 311–344.

Thomas, N.E., 1991. Geochemistry of groundwater in the Wilmot Park well field Fredericton, New Brunswick. MScE Thesis, University of New Brunswick, Department of Civil Engineering, Fredericton, NB, Canada.

Thomas, N.E., Kan, K.T., Bray, D.I., MacQuarrie, K.T.B., 1994. Temporal changes in manganese concentrations in water from the Fredericton Aquifer, New Brunswick. Ground Water 32 (4), 650–656.

Toride, N., Leij, F.J., van Genuchten, M.Th., 1995. The CXTFIT code for estimating transport parameters from laboratory or field tracer experiments, version 2.0. Research Report No. 137, US Salinity Laboratory, USDA, ARS, Riverside, California.

Valocchi, A.J., Roberts, P.V., Parks, G.A., Street, R.L., 1981. Simulation of the transport of ion-exchanging solutes using laboratory-determined chemical parameter values. Ground Water 19 (6), 600–607.

Violette, G.G. 1990. The application of a computer model to assess the potential effects of groundwater withdrawals from the Fredericton Aquifer, Fredericton, NB. MScE Thesis, University of New Brunswick, Department of Civil Engineering, Fredericton, NB, Canada.

von Gunten, U., Zobrist, J., 1993. Biogeochemical changes in groundwater-infiltration systems: column studies. Geochim. Cosmochim. Acta 57, 3895–3906.

von Gunten, H.R., Karametaxas, G., Krähenbühl, U., Kuslys, M., Giovanoli, R., Hoehn, E., Keil, R., 1991. Seasonal biogeochemical cycles in riverborne groundwater. Geochim. Cosmochim. Acta 55, 3597–3609.

Williamson, K., McCarty, P.L., 1976. A model of substrate utilization by bacterial films. J.Water Pollut. Control Fed. 48, 9–24.